AD-A242 867

OFFICE OF NAVAL RESEARCH

GRANT N00014-89-J-1178

R&T Code 413Q001-05

TECHNICAL REPORT NO. #39

DTIC
ELECTE
DEC 2 1991
S D
C

An Interface Enhanced Spectroscopic Ellipsometry Technique: Application to Si-SiO_2

by

V. A. Yakovlev and E. A. Irene
Department of Chemistry, CB# 3290
University of North Carolina
Chapel Hill, NC 27599-3290

Submitted to the
Journal of the Electrochemical Society

91-16637

Reproduction in whole or in part is permitted for any purpose of the United States Government.

This document has been approved for public release and sale; its distribution is unlimited.

91 11 27 039

SECURITY CLASSIFICATION OF THIS PAGE

REPORT DOCUMENTATION PAGE

1a. REPORT SECURITY CLASSIFICATION unclassified	1b. RESTRICTIVE MARKINGS
2a. SECURITY CLASSIFICATION AUTHORITY	3. DISTRIBUTION/AVAILABILITY OF REPORT Approved for public release; distribution unlimited.
2b. DECLASSIFICATION/DOWNGRADING SCHEDULE	
4. PERFORMING ORGANIZATION REPORT NUMBER(S) Technical Report #39	5. MONITORING ORGANIZATION REPORT NUMBER(S)
6a. NAME OF PERFORMING ORGANIZATION UNC Chemistry Department 6b. OFFICE SYMBOL (If applicable)	7a. NAME OF MONITORING ORGANIZATION Office of Naval Research (Code 413)
6c. ADDRESS (City, State and ZIP Code) CB# 3290, Venable Hall University of North Carolina Chapel Hill, NC 27599-3290	7b. ADDRESS (City, State and ZIP Code) Chemistry Program 800 N. Quincy Street Arlington, Virginia 22217
8a. NAME OF FUNDING/SPONSORING ORGANIZATION Office of Naval Research 8b. OFFICE SYMBOL (If applicable)	9. PROCUREMENT INSTRUMENT IDENTIFICATION NUMBER Grant #N00014-89-J-1178
8c. ADDRESS (City, State and ZIP Code) Chemistry Program 800 N. Quincy Street, Arlington, VA 22217	10. SOURCE OF FUNDING NOS. PROGRAM ELEMENT NO. / PROJECT NO. / TASK NO. / WORK UNIT NO.
11. TITLE (Include Security Classification) AN INTERFACE ENHANCED SPECTROSCOPIC ELLIPSOMETRY TECHNIQUE: APPLICATION TO $Si-SiO_2$	
12. PERSONAL AUTHOR(S) V. A. Yakovlev* and E.A. Irene	
13a. TYPE OF REPORT Interim Technical 13b. TIME COVERED FROM _____ TO _____	14. DATE OF REPORT (Yr., Mo., Day) November 1991 15. PAGE COUNT 31
16. SUPPLEMENTARY NOTATION Journal of the Electrochemical Society	
17. COSATI CODES FIELD / GROUP / SUB. GR.	18. SUBJECT TERMS (Continue on reverse if necessary and identify by block number)

19. ABSTRACT (Continue on reverse if necessary and identify by block number)

In this research we demonstrate an ellipsometry technique that is sensitive to the interfacial region between a dielectric film and substrate. Essentially, a film and substrate is immersed in a liquid that index matches to the film, thereby optically removing the film from the measurement. In addition, the use of spectroscopic and multiple angles of incidence ellipsometry provides sufficient specification of the interface parameters which along with the enhanced sensitivity to the interface, enables the optical measurement of the interfacial properties. Theoretical and experimental verification is provided along with application to the $Si-SiO_2$ interface.

20. DISTRIBUTION/AVAILABILITY OF ABSTRACT UNCLASSIFIED/UNLIMITED ☒ SAME AS RPT. ☐ DTIC USERS ☐	21. ABSTRACT SECURITY CLASSIFICATION Unclassified
22a. NAME OF RESPONSIBLE INDIVIDUAL Dr. Mark Ross	22b. TELEPHONE NUMBER (Include Area Code) (202) 696-4410 22c. OFFICE SYMBOL

DD FORM 1473, 83 APR EDITION OF 1 JAN 73 IS OBSOLETE.

SECURITY CLASSIFICATION OF THIS PAGE

An Interface Enhanced Spectroscopic Ellipsometry Technique: Application to $Si-SiO_2$.

V.A.Yakovlev* and E.A.Irene

Department of Chemistry
University of North Carolina at Chapel Hill
Chapel Hill, NC 25799-3290

* Institute of Crystallography, Acad. of Sci. USSR, Leninsky pr. 59 Moscow 117333 USSR

Abstract

In this research we demonstrate an ellipsometry technique that is sensitive to the interfacial region between a dielectric film and substrate. Essentially, a film and substrate is immersed in a liquid that index matches to the film, thereby optically removing the film from the measurement. In addition, the use of spectroscopic and multiple angles of incidence elllipsometry provides sufficient specification of the interface parameters which along with the enhanced sensitivity to the interface, enables the optical measurement of the interfacial properties. Theoretical and experimental verification is provided along with application to the $Si-SiO_2$ interface.

Accession For
NTIS GRA&I
DTIC Tab
Unannounced
Justification
By
Distribution/
Availability Codes
Dist | Avail and/or Special
A-1

#39 submitted to J. Electrochem Soc.

Introduction.

The performance of thin film microelectronics devices is highly dependent on the nature and perfection of the interface between substrate and film. Of particular technological interest is the Si-SiO_2 interface, where electronic states are located that greatly alter device performance. Thus, the characteristics of devices utilizing this interface can be influenced by roughness, thickness and composition of the thin interfacial transition region only a few nm thick in between the crystalline Si substrate and the amorphous and stoichiometric SiO_2. Much work has been done to study the Si-SiO_2 interface using a variety of techniques such as transmission electron microscopy (1-4), low-energy electron diffraction (5), Auger spectroscopy (6), x-ray photoelectron spectroscopy (7), scanning tunneling microscopy(8), infrared spectroscopy (9), ellipsometry (10-19) and others (20-29). Emerging from these studies are not only commonly agreed upon points, viz. that the interfacial region is different from both film (overlayer) and substrate and that a variation of interfacial properties is a strong function of processing, but also considerable controversy about the detailed nature of the interface. At least part of the controversy stems from the fact that various measurement techniques probe different aspects of the interface and that the techniques themselves are implicated in interfacial changes, e.g. removal of the overlayer by etching and/or bombardment using energetic beams. Spectroscopic

ellipsometry, SE, is a non-destructive yet powerful tool for studying film and surface properties. In principle ellipsometry can take advantage of the transparency of an overlayer such as SiO_2 in the visible light region, in order to probe the interface region. In practice however an accurate characterization of the ultra-thin interface transition layer is complicated by the inability to discriminate the optical contributions of the relatively thick overlayer and the thin transition layer from the measured ellipsometric parameters. Notwithstanding the difficulties, a number of studies(10-19) have applied ellipsometry to probe the Si-SiO_2 interface. In a pioneering investigation Taft and Cordes (10) performed single-wavelength (λ=546.1 nm) ellipsometry measurements on thermally oxidized silicon and estimated that the interface layer is 0.6 nm thick with an index of refraction of 2.8. In an effort to enhance the sensitivity of ellipsometry to the transition region, it was shown (29) that when the wavelength of the incident light is adjusted to the antireflection condition (where the s or p polarized component of the incident light is transmitted through to the substrate with minimum reflected intensity), the interface layer can strongly influence the antireflection interference condition established in the top layer, thereby yielding an enhanced sensitivity to the thickness and the optical properties of the transition layer. In addition to the choice of λ, the antireflection condition depends on the optical path length (product of index, n and thickness L) through the overlayer. For SiO_2 on Si, a thickness in the range

of about 70-160 nm in the visible-near UV spectroscopic region is appropriate (30-31). Using this technique Aspnes and Theeten(11,12) performed spectroscopic ellipsometry, SE, measurements on thermally oxidized Si with SiO_2 thicknesses of 120-160 nm and found an interface transition region of about 0.7 nm that consists of atomically mixed Si and O with average stoichiometry $SiO_{0.4}$. With the conclusion that the processing effects the interface region and the importance of ultra-thin (less than 25 nm) SiO_2 films and other dielectrics, questions about the interface region remain. Kalnitsky et al.(15) and Chongsawangvirod et al.(16) performed single-wavelength, high-accuracy nulling ellipsometry measurements on very thin SiO_2 films on Si and found that the refractive index of the SiO_2 film substantially increases with decreasing film thickness. From an analysis using a single film optical model, these authors concluded that the observed rise of n(L) with decreasing film thickness, L, includes both a real effect of an SiO_2 optical density increase near the Si-SiO_2, and an apparent effect due to the existence and increasing importance (as the fraction of the interface increases) of a higher optical density interface layer. These measurements were not able to decouple the two effects. Application of multiple angles of incidence, MAI, ellipsometry has the advantages of improving the precision of single wavelength ellispometry and reducing the intercorrelation of unknown parameters. Chao et al.(18) used MAI ellipsometry with three interfacial models (abrupt, linear and exponential) to fit the ψ,Δ data from SiO_2 thermally grown on Si.

For oxides less then 15 nm, they found that the refractive index increases rapidly with a decrease in thickness. The abrupt interface model was found to be the most appropriate model for the Si-SiO_2 interface with the SiO_2 overlayer thickness in the range 5-40 nm. Nevertheless, the MAI measurements alone, without spectroscopic ellipsometry, SE, could not provide enough sensitivity to obtain the composition of the interface. A recent and complete ellipsometric investigation of the thermally grown SiO_2 on Si system in the 3-325 nm film thickness range was performed by Jellison using a two-channel spectroscopic polarization modulation ellipsometer(19) in the spectral energy range 1.48-5.16 eV at one angle of incidence. A two layer optical model was used (interface and SiO_2 layers) to fit the experimental data and a single term Sellmeier approximation was used for SiO_2, and the interface layer was modeled as a mixture of fused SiO_2 and crystalline Si. It was found that the refractive index of the SiO_2 increases with decreasing film thickness, while the interfacial layer thickness decreases with decreasing film thickness. For SiO_2 film thicknesses less then 25nm it was concluded that the interface layer is less then a few tenths of a nm and it was not included in the fitting calculations.

In this paper we present a novel enhanced sensitivity spectral and variable angle of incidence immersion ellipsometry technique for studying dielectric-semiconductor interfaces and demonstrate its advantage on the Si-SiO_2 system. The main feature of this technique is that spectroscopic and variable angle of incidence

measurements are performed in a transparent liquid ambient that has optical properties very close to the optical properties of the dielectric overlayer. In this way the overlayer is "optically" (non-destructively) eliminated and the probing beam becomes highly sensitive to the interface properties. By collecting spectroscopic scans at several angles of incidence in the vicinity of Brewster's angle, the interface layer can be over determined. A variable angle of incidence immersion cell was constructed for this purpose.

The Optical Model

The Interface Layer. The transition from crystalline Si to bulk amorphous SiO_2 includes at least two different regions. First there is a region from the c-Si where the long-range crystalline order of c-Si disappears. The characteristic range for this zone is small and about 0.2-2nm. Second there is a longer range region extending tens of nm into the amorphous SiO_2 where mechanical stress, density and refractive index relax to the bulk SiO_2 film values. This transition region has a complicated structure which is thought to consist of two parts: the "physical" interface and the "chemical" interface. The "physical" interface consists of a mixture of substrate and overlayer compositions, and can represent microroughness(26) or inclusions. Recent high-resolution transmission electron microscopy(21), x-ray scattering(25,27) and photoemission(28) studies indicate the presence of highly oriented SiO_2 microcrystallites, such as crystobalite or tridymite, embedded

in an amorphous connected phase. The existence of the crystalline inclusions decreases the interfacial energy and allows the long-range order of c-Si to decay gradually into the amorphous phase. The "Chemical" interface is the actual chemical transition zone and consists of a new chemical compound or mixture of compounds that occurs during film formation. In the Si-SiO_2 system this interface is usually treated as a suboxide, SiO_x, with $0<x<2$, and with optical properties dependant on x (32).

The complicated transition layer extending from tenths of a nm to much less than $\lambda/4$, where λ is the wavelength of probing beam, influences the polarization of the incident light beam. In order to represent this region optically, we use a uniform dielectric function in which the interface transition region is considered to be a homogeneous layer with an effective thickness L_{inf} and an effective dielectric function ϵ_{eff}, as can be calculated by the Bruggeman effective medium approximation, BEMA, where the dielectric properties of all of the interfacial layer constituents are known a priori.

The SiO_2 Overlayer. It is reported that ultra-thin (less than 25 nm) SiO_2 films display a gradual decrease in the refractive index profile from the interface to the bulk SiO_2 with specific values that depend on the preparation method(16-19). It is therefore expedient to model the thin films as optically inhomogeneous structures with a decreasing refractive index towards the outer surface. Consequently, it is very difficult to choose an immersion

liquid which will adequately match this layer; and for spectroscopic measurements the dispersion of both the SiO_2 overlayer and the immersion liquid will alter an initial match. Nevertheless, as we will show below, it is possible to minimize the errors associated with the inhomogeneity by using a previously estimated thickness for the overlayer.

For an ultra-thin homogeneous film we write the Drude-Archer expression for the relation between the phase shift Δ of the reflected light and the thickness L of the film as:

$$\Delta = \overline{\Delta} + C_{\Delta} L \quad (1)$$

where $\overline{\Delta}$ is the change in the phase shift for a bare substrate and

$$C_{\Delta} = (n_o^2 - n_f^2)\, f(\lambda, \phi, n_o, n_f, n_s, k_s) \quad (2)$$

where ϕ is the angle of incidence, n_o , n_f , n_s are the refractive indices of the ambient, the film and the substrate, respectively, and k_s is the absorption index. (Analogous expressions can be written for ψ).

We write the refractive index of the overlayer as a function of film thickness:

$$n_f(L) = n_f + \delta n_f(L) \quad (3)$$

where n_f is an average refractive index and $\delta n_f(L) << n_f$ characterizes the refractive index gradient. If the refractive index of the immersion liquid is equal to n_f at some wavelength, then the uncertainty, $\delta\Delta$, connected with the gradient $\delta n_f(L)$ is given as:

$$\delta\Delta = 2\delta n_f(L)\, L \cdot f(\lambda, \phi, n_o, n_f, n_s, k_s) \quad (4)$$

Taking into account dispersion of the refractive indexes of the overlayer, $\delta n_f(\lambda)$, and the immersion liquid, $\delta n_o(\lambda)$, we obtain:

$$\delta\Delta \sim \delta n_f L \cdot f \quad (5)$$

with f the function above and where:

$$\delta n_f = \delta n_f(L) + \delta n_f(\lambda) \quad (6)$$

If the thickness of the overlayer L is known with precision $\delta L \ll L$, for example from measurements in air, then eqn(5) is much smaller than 1 and therefore negligible. Thus, if the refractive index of the ambient is close to the average refractive index of the overlayer, n_f, and the overlayer thickness is known, then it is possible to describe the overlayer as a homogeneous film.

The refractive index of the transparent overlayer was determined from a single term Sellmeier approximation:

$$n^2(L) = 1 + \frac{A(L)\,\lambda^2}{\lambda^2 - \lambda_o^2(L)} \quad (7)$$

where the parameters A(L) and $\lambda_o(L)$ are dependent on the overlayer thickness and preparation conditions(19) with A=1.1 and λ_o = 92.3nm for thick SiO_2 films (more than 200 nm), but A=1.15 for a 20 nm thick thermally grown (1000° C) film.

Since n is dependent on the thickness of the film, the use of immersion liquids with different refractive indexes corresponding to the average refractive indexes of the films under investigation gives the possibility of improving the accuracy of the method.

The Ambient. The ideal immersion liquid should be non reactive and transparent over a wide spectral range. Both the refractive index and the dispersion must correspond to the average refractive index of the overlayer and some values are given in Table I (42). The refractive indices for the immersion liquids were calculated from a three term Cauchy dispersion formula, taking into account temperature:

$$n_o = n_\infty + \frac{a}{\lambda^2} + \frac{b}{\lambda^4} + \frac{\partial n}{\partial T}\Delta T \quad (8)$$

Using a mixture of different liquids it is possible to cover a range of refractive indexes of the ambient near to that for SiO_2. Figure (1) shows the spectral dependencies of the refractive index of pure carbon tetrachloride, CCl_4, benzene, C_6H_6, and mixtures(33). Both CCl_4 and C_6H_6 are nonpolar organic liquids that do not interact with SiO_2. Also in Figure 1 is shown the spectral dependencies of the refractive index of bulk and thin film SiO_2 calculated using the data of Table I and eqn(7).

Analysis. In order to analyze the sensitivity of the technique, we consider the complicated substrate-interface-inhomogeneous overlayer structure to be a two film system with interface and overlayer thicknesses L_{inf} and L_{ov}, respectively and depicted in Figure 2. The interface and the overlayer are characterized by an effective dielectric function ϵ_{inf} of the interface and an average refractive index n_{ov} of the overlayer. The complex reflection

coefficient, ρ, for the system is given by:

$$\rho = \tan\Psi \exp(i\Delta) = \rho(\lambda, \phi, n_o, n_{ov}, n_s, k_s, e_{inf}, L_{ov}, L_{inf}) \quad (9)$$

The maximum change in ρ, $\delta\rho/\rho$, is the condition of optimum sensitivity in the measurables, Δ, Ψ. It is desirable to determine the optimum sensitivity in terms of the controllable parameters, ϕ and λ. From the analytical solution for optimized ellipsometric measurements of interfaces with $L_{inf} << \lambda/4$ in thin film structure(31), it was shown that the condition of $\delta\rho/\rho$ divergence or maximum sensitivity is:

$$r_{01}^{p(ands)} + r_{12}^{p(ands)} \exp(-2i\beta) = 0 \quad (10)$$

where the r's are the Fresnel reflection coefficients with subscripts corresponding to the interface between the numbered media in Figure 2 and β is given as:

$$\beta = \frac{2\pi L_{ov}}{\lambda}\sqrt{(n_{ov}^2 - n_o^2 \sin^2\phi)} \quad (11)$$

It should be observed that the properties of the interface do not influence the best sensitivity conditions.

If the refractive index of the ambient is close to the index of the overlayer, i.e. $n_o \approx n_{ov}$, then $r_{01} \approx 0$. The optimum sensitivity condition from eqn (10) becomes r_{12} or, taking into account $n_o \approx n_{ov}$, $r_{02} \approx 0$. For the p wave this condition is equal to a minimum of the ellipsometric angle, $\Psi(\phi,\lambda)$(31).

Our approach to find the proper spectral range and angles of incidence is to simulate $\Psi(\phi,\lambda)$ and $\Delta(\phi,\lambda)$ dependencies using the model in Figure 2 for the Si-SiO_2 system with the following

assumptions: a. crystalline Si substrate with known dielectric function(41); b. interface microroughness (see Figure 2) with effective height of 0.2nm and composition of 50% c-Si and 50% suboxide SiO_x, with x = 0.4 and BEMA was used to calculate a dielectric function of the mixture; c. interface suboxide transition zone of 0.6nm composed of $SiO_{0.4}$; d. SiO_2 overlayer with an average refractive index $n_{ov}(L)$ calculated from eqn(7); e. an air or pure CCl_4 ambient with refractive index n_o calculated from eqn(8).

Fig. 3 shows simulation results for the air-20nm SiO_2-Si system with and without a 0.7nm interface in terms of $\Psi(E)$ and $\Delta(E)$ where E is the energy of probing light in the energy range 2.5-4.0 eV. It is clearly seen that for the air ambient there is very low sensitivity in both Δ and Ψ to the presence of an interface layer different from SiO_2. Figure 4 shows the analogous simulation of the CCl_4-20 nm SiO_2-Si system. The interface sensitivity of Δ is drastically increased using the CCl_4 ambient. The enhancement in sensitivity is shown better in Fig.5 which plots the relative interface sensitivity $\delta\Delta(E) = \Delta_0(E) - \Delta_{inf}(E)$ for air and CCl_4 ambients. $\Delta_0(E)$ and $\Delta_{inf}(E)$ were calculated without and with an interface layer, respectively. The sensitivity of Δ to the presence of an interfacial layer is increased more than an order of magnitude with parameters at optimum sensitivity, but the Ψ sensitivity is low. However, changing ϕ to 78° for the same system enhances the ψ sensitivity to the interfacial layer and this is shown in Figs. 5 and 6.

Correlation of Parameters and Measurement Errors. Film thicknesses and optical parameters of ultra-thin films are highly correlated. This is due to the fact that the optical path through a material is measured and the optical path is essentially the product of thickness and complex index. In terms of the ellipsometric measurables we can write this relationship as:

$$\frac{\partial \Psi}{\partial L} \sim \frac{\partial \Psi}{\partial n} \text{ and } \frac{\partial \Delta}{\partial L} \sim \frac{\partial \Delta}{\partial n} \quad (12)$$

Spectroscopic (as opposed to single wavelength) ellipsometry measurements at a fixed angle of incidence helps to decrease the correlation, but does not overcome this problem(34,35), especially when the number of unknown parameters is more than two. In order to obtain more information about the properties of the interface, it is useful to use both SE and MAI measurements to eliminate the correlation between the thickness of the interface and its optical parameters. For this purpose we designed a variable angle of incidence immersion cell (Figure 7) in which to perform MAI SE measurements.

A problem with the enhanced sensitivity measurements is the corresponding increasing influence of errors to optimized conditions. A high value of $\partial\Delta/\partial\phi$ will increase the sensitivity of Δ not only to changes of the optical parameters of the system, but also to any errors in the angle of incidence, ϕ. For our high sensitivity configurations ($\Psi \approx 0°$) the largest contribution to $\delta\Delta_{err}$ comes from the angle of incidence error $\delta\phi$(31). Therefore, in order to obtain more reliable values for the parameters (or to

determine values for a larger number of parameters), an accurate measurement of ϕ is important. We paid special attention to the design of the variable angle immersion cell (autocollimation techniques and small apertures were allowed for in our design and used for alignment), and to the alignment of the cell windows, in order to obtain a precision of 0.01° in ϕ in liquid in the range 67°-90°.

Inversion Process. In order to find unknown parameters of the modeled interface, we used the Marquardt non-linear best-fit algorithm which minimizes the value of the error function:

$$Q = \sum_{i,j} [(\Delta_{i,j}^{cal}(\phi_i, E_j, P) - \Delta_{i,j}^{exp})^2 + (\Psi_{i,j}^{cal}(\phi_i, E_j, P) - \Psi_{i,j}^{exp})^2] \quad (13)$$

where P is a vector of N unknown interface parameters and E_j is the energy, and the superscripts cal and exp refer to calculated and experimentally derived values. Δ^{cal} and Ψ^{cal} are the values obtained using the vector P, the Fresnel formulas(36) and a matrix algorithm for the multilayer system complex reflection coefficient. Optical parameters for the immersion liquid and SiO_2 overlayer included in the fitting procedure were calculated from dispersion equations (7) and (8). BEMA was used to calculate the effective dielectric function for a mixture of constituents with known optical properties. Volume fractions of the constituents have been included as unknown parameters.

The calculation gives the vector P when an initial guess, P^o, is input, i.e. the program returns a value of P at the local

minimum of Q, near the initial value. In addition, correlation between the fitting parameters are expressed in terms of the correlation matrix of the derivatives $\partial\Psi/\partial p_a$, $\partial\Delta/\partial p_a$ and a 95% confidence limit was used to calculate errors in the fitting parameters.

Experimental Procedures

A commercially available vertical ellipsometer bench was modified to become rotating analyzer spectroscopic ellipsometer (the essential features were previously described(37) and calibrated according to a published procedure(38). Calibration was performed on a sample with $\Delta\approx90°$ (Si wafer with thermally grown SiO_2 film) both in air and in the immersion cell in liquid. The difference between the calibration parameters (polarizer P_{off} and analyzer A_{off} offsets, normalization factor η) were negligible.

A fused silica immersion cell, as shown in Fig.7, has been designed for the variable angle of incidence and spectroscopic measurements. The main feature of the cell is that the two optically flat and annealed fused silica plates, serving as the entrance and exit windows, are connected rigidly to the polarizer and analyzer arms, but not to the cell. The angular orientation of the windows was adjusted at the straight-through position of the ellipsometer (ϕ=90°), in order to avoid any deviation of the incident light beam. The windows must be orthogonal to the beam for the immersion measurements, otherwise the media with different

indexes of refraction on each side of the windows will alter the direction of the beam, hence the angle of incidence by an amount proportional to the amount of deviation from orthogonal. Two fitted metallic tubes in each arm permit some lateral movement of the window position without a change of the window tilt. The cell is rigidly attached to a stage and connected to the tubes using flexible tubing that are inert to the immersion liquids. A change of ϕ in the range of 67°-90° is possible while maintaining the window alignment precision during the immersion measurements.

Commercially obtained device quality silicon wafers of (100) orientation, p-type in the 2 Ω cm resistivity range were cleaned prior to oxidation using a slightly modified RCA cleaning procedure (39). The samples were thermally oxidized to about 20nm at 800°C in a fused silica tube furnace in clean dry oxygen which yielded MOS quality SiO_2 films on Si.

Results and Discussion

As was discussed above, the method requires an estimation of the overlayer thickness. One layer (substrate-overlayer) and two layer (substrate-interface-overlayer) models have been used to analyze the spectroscopic ellipsometry scans of the thin 25nm SiO_2 on Si samples in air. From these measurements in air, it was found that the difference in the minimum error function, Q, for one and two layer models was negligible for our samples, indicative of the low interface sensitivity. These measurements yield a good estimate of the overlayer thickness to a precision of better than

0.5%. The refractive index of the film was calculated from the dispersion relation, eqn(7), with parameters A(L) and $\lambda_o(L)$ taken from Table I for a film thickness 25 nm. Immersion measurements were performed in pure CCl_4 at 20°C.

Carbon tetrachloride becomes nontransparent at energies higher ~4 eV. Thus the upper limit of the spectral range was chosen to be 4eV. The precision of rotating analyzer ellipsometry without using an achromatic compensator falls significantly when Δ approaches 180° or 0°(40). To avoid this situation, we have used 2.5 eV as the lower energy limit where Δ is more than 20° (see Figure 4). Therefore, Δ is restricted to $20°<\Delta<160°$ in the spectral range 2.5-4.0 eV for the measurements in the immersion liquid at the angles of incidence ϕ = 70°-80° (see Figs. 4 and 6).

Fig.8 shows the experimental data with the best-fit curves $\Psi(E)$, $\Delta(E)$ for the scan in CCl_4 at ϕ = 72°. For the calculation of the best fit curves, the interface was modeled as a two-layer system consisting of a layer of microroughness and a suboxide, SiO_x, layer. The microroughness was modeled as a mixture c-Si and suboxide SiO_x. The dielectric function of SiO_x was calculated using the BEMA and supposing that SiO_x is a mixture of a-Si and the SiO_2 overlayer and calculated by eqn (7). We also allowed the previously estimated value of the overlayer thickness to be a variable parameter, and to change it by ≈ 2% from the initial value obtained from the scan in air. This procedure improved the fit. The minimization of the error function (eqn(13)) for the sets of the experimental data at ϕ = 72° and 75° by the Marquardt algorithm

gives both the thicknesses of the microroughness layer L_{mr}, the suboxide transition layer L_u and the volume fraction of the interface constituents. So, for the ~ 25nm thick SiO_2 film L_{mr} = .22±0.04 nm, 40% c-Si, 60% SiO_x, x = 0.33±0.05, L_u = 0.63±0.08 nm with an overlayer thickness L_{ov} = 24.1±0.06nm. Fig. 8 shows satisfactory agreement between the experimental and the best-fit curves and our results are in substantial agreement with the variety of studies referenced above.

A general enhanced sensitivity spectral and variable angle of incidence immersion ellipsometry technique has been developed for studying dielectric-semiconductor interfaces. Specifically, a high sensitivity of this technique for the Si-SiO_2 system with thin SiO_2 films has been demonstrated. Detailed investigations of the Si-SiO_2 interface properties with various process conditions are in progress.

Acknowledgments.

This research was supported in part by the Office of Naval Research, ONR.

REFERENCES

1. J.Blanc, C.J.Buiocchi, M.S.Abrahams, and W.E.Ham, Appl. Phys. Lett., 30, 120 (1977).

2. O.J.Krivanek and J.H.Mazur, Appl. Phys. Lett., 37, 392 (1980).

3. N.M.Ravindra, D.Fathy, J.Narayan, J.K.Srivastava, and E.A.Irene, Materials Lett., 4, 337 (1986).

4. N.M.Ravindra, D.Fathy, J.Narayan, J.K.Srivastava, and E.A.Irene, J. Mater. Res., 2, 216 (1987).

5. P.O.Hahn and M.Henzler, J. Appl. Phys., 52, 4122 (1981).

6. Min-Shen Lei and Zhi-Chen Wang, Phys. Stat. Sol.(b), 120, 189 (1983).

7. F.J.Grunthaner and J.Maserjian, in " The Physics of SiO_2 and its Interfaces", Proceedings of the International Topical Conference, Yorktown Heights, NY, 1978, edited by S.T.Pantelides (Pergamon, New York,1978), p.384.

8. A.H.Carim, M.M.Dovek, C.F.Quate, R.Sinclair, and C.Vorst, Science, 237, 630 (1987).

9. I.W.Boyd, J.I.B.Wilson, J. Appl. Phys., 62, 3195 (1987).

10. E.A.Taft and L.Cordes, J. Electrochem. Soc., 126, 131 (1979).

11. D.E.Aspnes and J.B.Theeten, Phys. Rev. Lett., 3, 1046 (1979).

12. D.E.Aspnes and J.B.Theeten, J.Electrochem.Soc., 127, 1359 (1980).

13. G.E.Jellison, Jr. and F.A.Modine, J. Opt. Soc. Am., 72, 1253 (1982).

14. Ph. Ged, A.Vareille, and D.Bois, Thin Solid Films, 91, 327 (1982).

15. A.Kalnitsky, S.P.Tay, J.P.Ellul, S.Chongsawangvirod, J.W.Andrews, and E.A.Irene, J. Electrochem. Soc., 137, 234 (1990).

16. S.Chongsawangvirod, E.A.Irene, A.Kalnitsky, S.P.Tay, and J.P.Ellul, J. Electrochem. Soc., 137, 3536 (1990).

17. V.Nayar, C.Pickering, and A.M.Hodge, Thin Solid Films, 195, 185 (1991).

18. T.S.Chao, C.L.Lee, and T.F.Lei, J. Electrochem. Soc., 138, 1756

(1991).
19. G.E.Jellison, Jr., J. Appl. Phys., 69, 7627 (1991).

20. P.J.Grunthaner, M.H.Hecht, F.J.Grunthaner, and N.M.Jonson, J. Appl. Phys., 61, 629 (1987).

21. A. Ourmazd, D.W.Taylor, J.A.Rentschler, and J.Belk, Phys. Rev. Lett., 59, 213 (1987).

22. A. Ourmazd, P.H.Fuoss, J.Belk, and J.F.Mosser, Appl. Surf. Sci., 41/42, 365 (1987).

23. W.Braun and H.Kuhlenbeck, Surf. Sci., 180, 279 (1987).

24. F.J.Himsel, F.R.McFeely, A.Taleb-Ibrahim, J.A.Yarmoff, and G.Hollinger, Phys. Rev. B., 38, 6084 (1988).

25. P.H.Fuoss, L.J.Norton, S.Brennan, and A.Fischer-Colbrie, Phys. Rev. Lett., 60, 600 (1988).

26. J.Sune, I.Placecia, N.Barniol, E.Farres, and X.Aymerich, Surf. Sci., 208, 463 (1989).

27. I.Harisawa, K.Akimoto, T.Tatsumi, J.Mizuki, and J.Matsui, J. Cryst. Growth, 103, 150 (1990).

28. M.Niwano, H.Katakura, Y.Takeda, Y.Takakuwa, N.Miyamoto, A.Hiraiwa, and K.Yagi, J. Vac. Sci. Technol. A, 9, 195 (1991).

29. J.B.Theeten, D.E.Aspnes, and R.P.H.Chang, J. Appl. Phys., 49, 6097 (1978).

30. S.A.Alterovitz, G.H.Bu-Abbud, J.A.Woollam, and D.C.Liu, J. Appl. Phys., 54, 1559 (1983).

31. S.A.Alterovitz, G.H.Bu-Abbud, and J.A.Woollam, Thin Solid Films, 128, 183 (1985).

32. G.Zuther, Phys. St. Sol.(a), 59, K109 (1980).

33. P.Perez, T.E.Block, and C.M.Knobler, J. Chem. and Eng. Data, 16, 333 (1971).

34. G.H.Bu-Abbud and N.M.Bashara, Appl. Optics, 20, 3020 (1981).

35. G.H.Bu-Abbud, N.M.Bashara, and J.A.Woollam, Thin Solid Films, 138, 27 (1986).

36. R.M.A.Azzam and N.M.Bashara, Ellipsometry and Polarized Light, North-Holland, Amsterdam, 1977.

37. X.Liu, J.W.Andrews, and E.A.Irene, J. Electrochem. Soc., 138,

1106 (1991).
38. J.M.M. de Nijs, A.H.M.Holtslag, A.Hoeksta, and A. van Silfhout, J. Opt. Soc. Am. A, 5, 1466 (1988).

39. W.Kern and D.A.Puotinen, RCA Rev., 31, 187 (1970).

40. D.E.Aspnes, J. Opt. Soc. Am., 64, 639 (1974).

41. D.E.Aspnes, A.A.Studna, Phys. Rev. B: Condensed Matter, 27, 985 (1983).

42. "Techniques of Chemistry", Ed. A. Weissberger, Vol.II Organic Solvents, Ed. J.A. Riddick and W.B. Bunger, Wiley_Interscience, NY, 1970.

Table I Refractive Index Values for Immersion Liquids

SiO_2 Thk (nm)	Refractive Index SiO_2[16]	Liquid	Refractive Index Liquid[42]	dn/dT
20	1.465-1.475	Carbon Tetrachloride	1.460	0.00055
10	1.485-1.495	Glycerine Toluene	1.475 1.497	0.00056
7	1.515-1.525	Benzene	1.501	0.00063

List of Figures

Fig. 1. The refractive index versus photon energy for pure carbon tetrachloride (CCl_4), and benzene (C_6H_6), and mixtures, along with bulk and thin-film SiO_2.

Fig. 2. Model for the substrate-interface-overlayer-ambient system.

Fig. 3. Calculated ellipsometric parameters ψ and Δ vs photon energy for a system with and without a distinct interface layer in ambient air and ϕ=72°.

Fig. 4. Calculated ellipsometric parameters ψ and Δ vs photon energy for a system with and without a distinct interface layer in carbon tetrachloride with ϕ=72°.

Fig. 5. Difference between the calculated ellipsometric parameters ψ and Δ vs photon energy for a system with and without a distinct interface layer in ambients air and CCl_4.

Fig. 6. Calculated ellipsometric parameters ψ and Δ vs photon energy for a system with and without a distinct interface layer in a carbon tetrachloride ambient with ϕ=78°.

Fig. 7. Configuration of the variable angle of incidence immersion cell.

Fig. 8. The experimental and calculated best-fit ellipsometric parameters Ψ and Δ for the CCl_4 ambient.

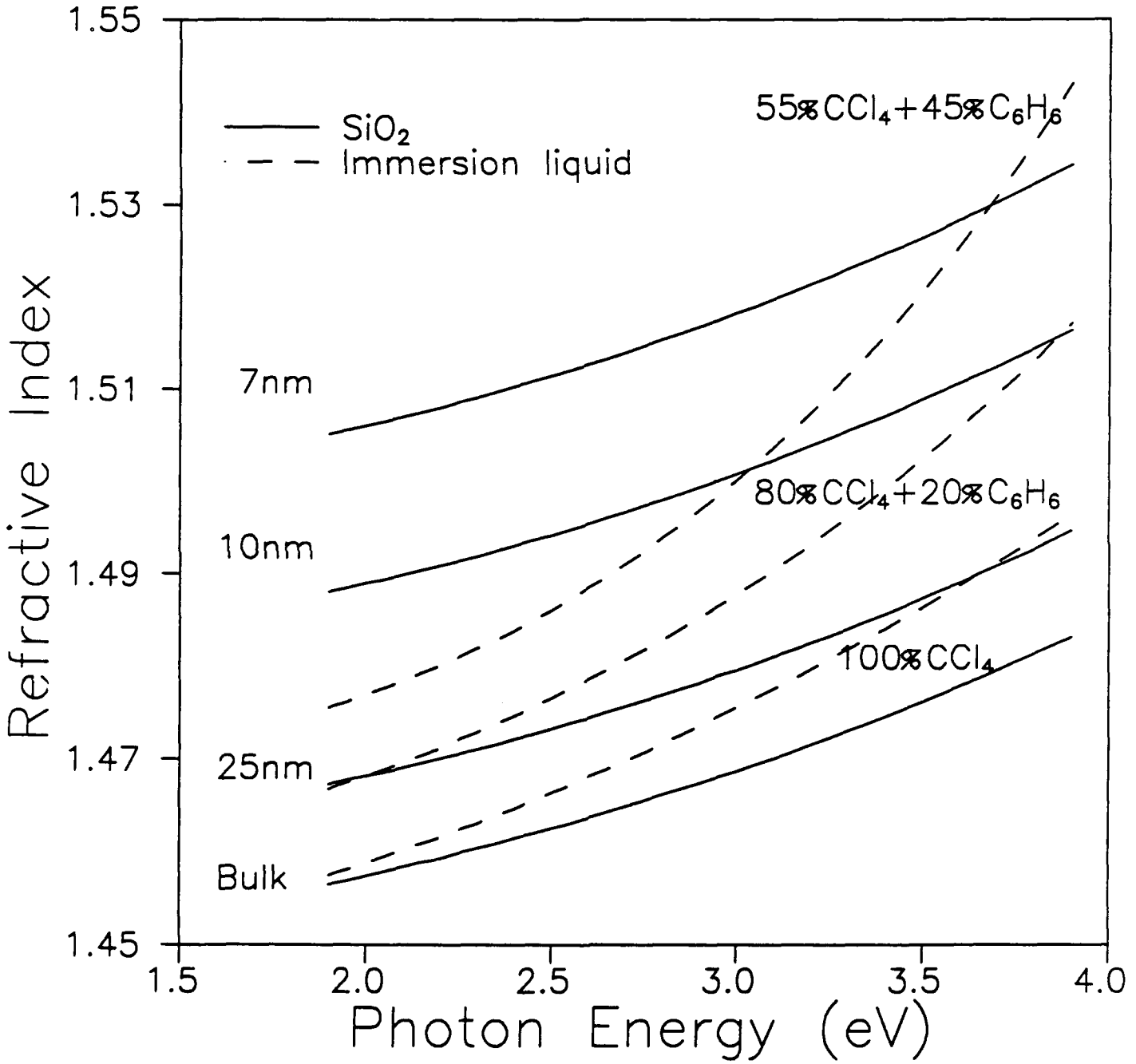

1.55
1.53
1.51
1.49
1.47
1.45
Refractive Index
SiO2
Immersion liquid
55% CCl4 + 45% C6H6
80% CCl4 + 20% C6H6
100% CCl4
7nm
10nm
25nm
Bulk
1.5
2.0
2.5
3.0
3.5
4.0
Photon Energy (eV)

Fig 1.

Optical Model

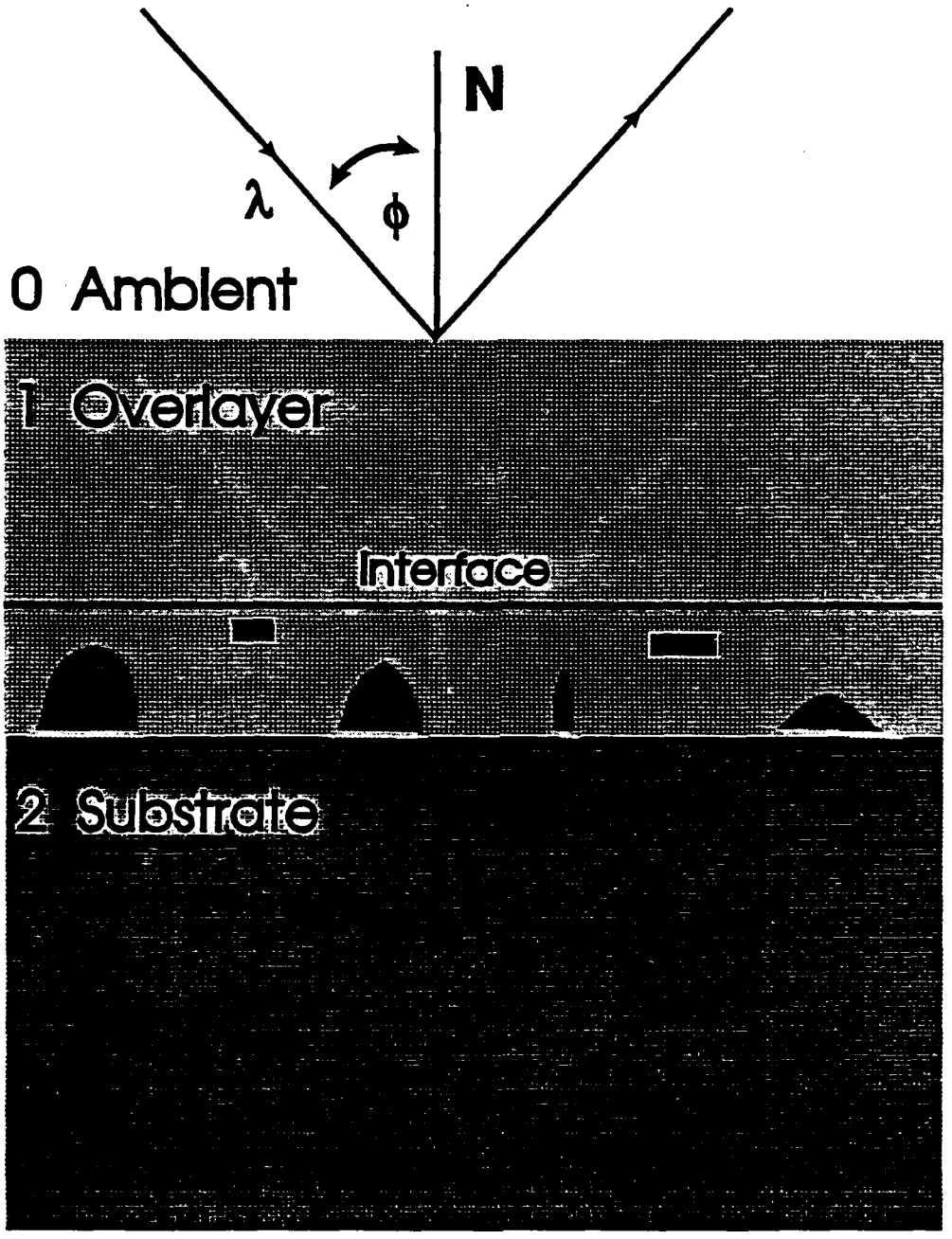


Fig 2

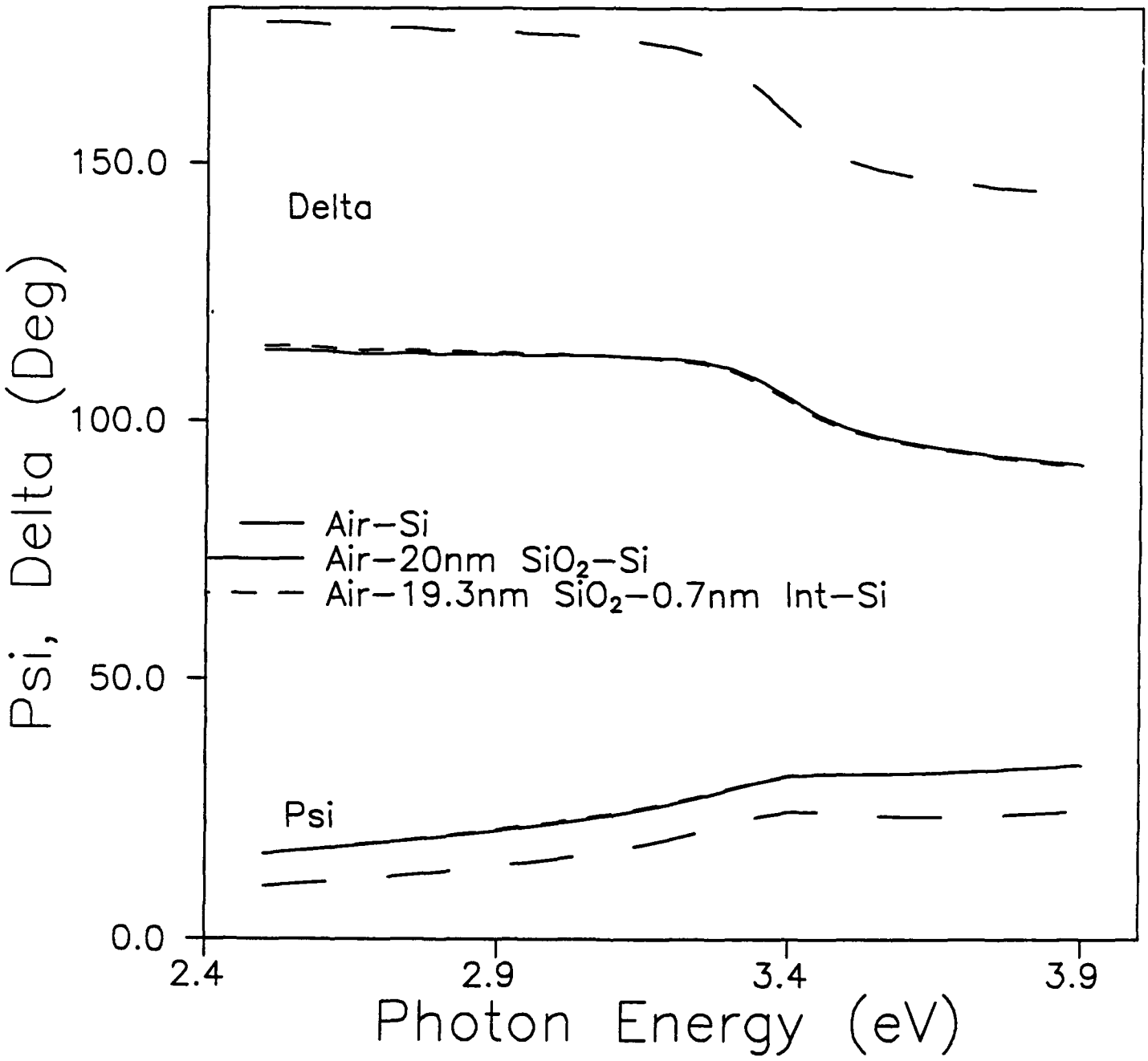

150.0
100.0
50.0
0.0
Psi, Delta (Deg)
Delta
Psi
Air–Si
Air–20nm SiO2–Si
Air–19.3nm SiO2–0.7nm Int–Si
2.4
2.9
3.4
3.9
Photon Energy (eV)

Fig 3

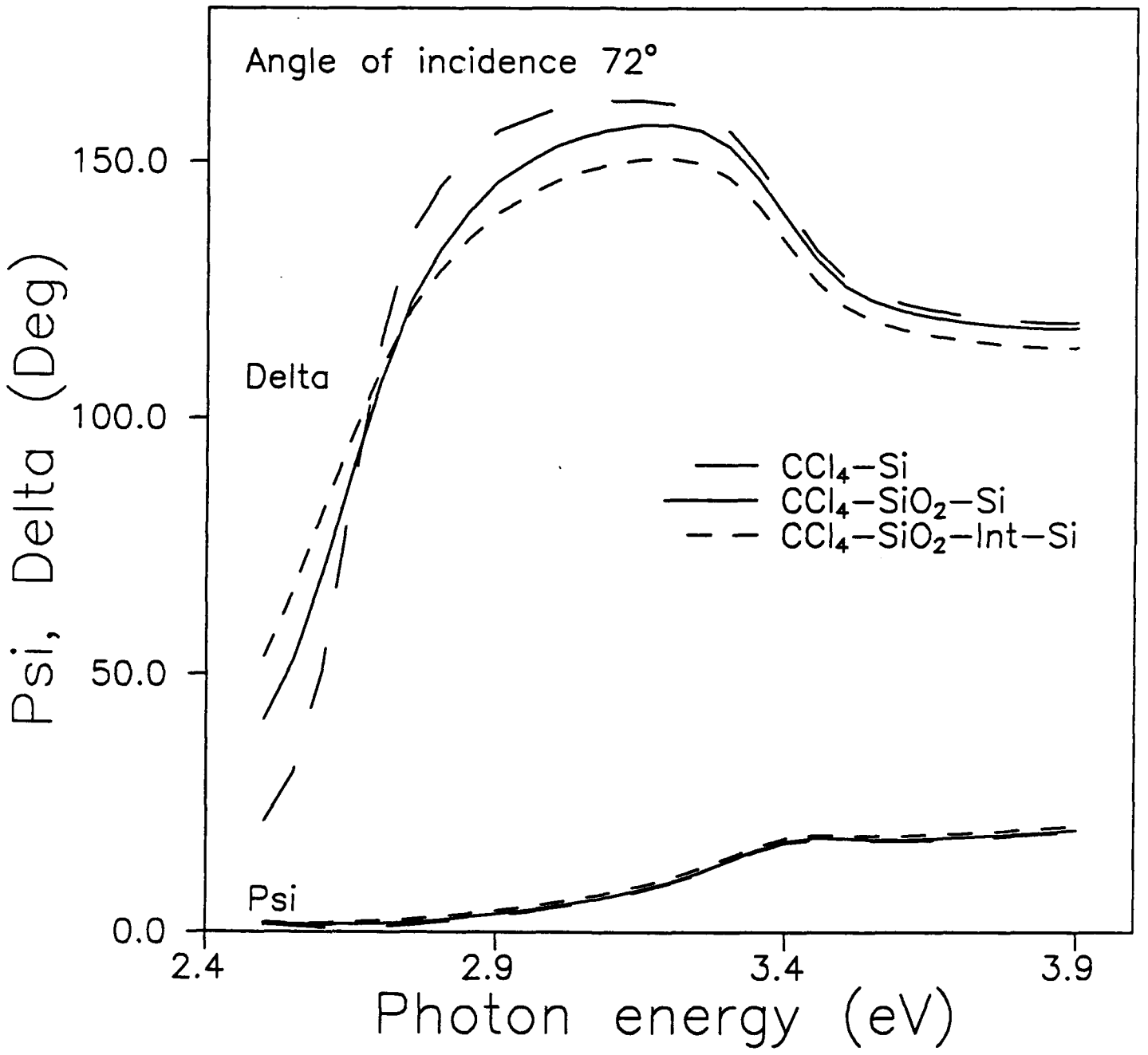

Angle of incidence 72°
150.0
100.0
50.0
0.0
Psi, Delta (Deg)
Delta
Psi
CCl4–Si
CCl4–SiO2–Si
CCl4–SiO2–Int–Si
2.4
2.9
3.4
3.9
Photon energy (eV)

Fig 4

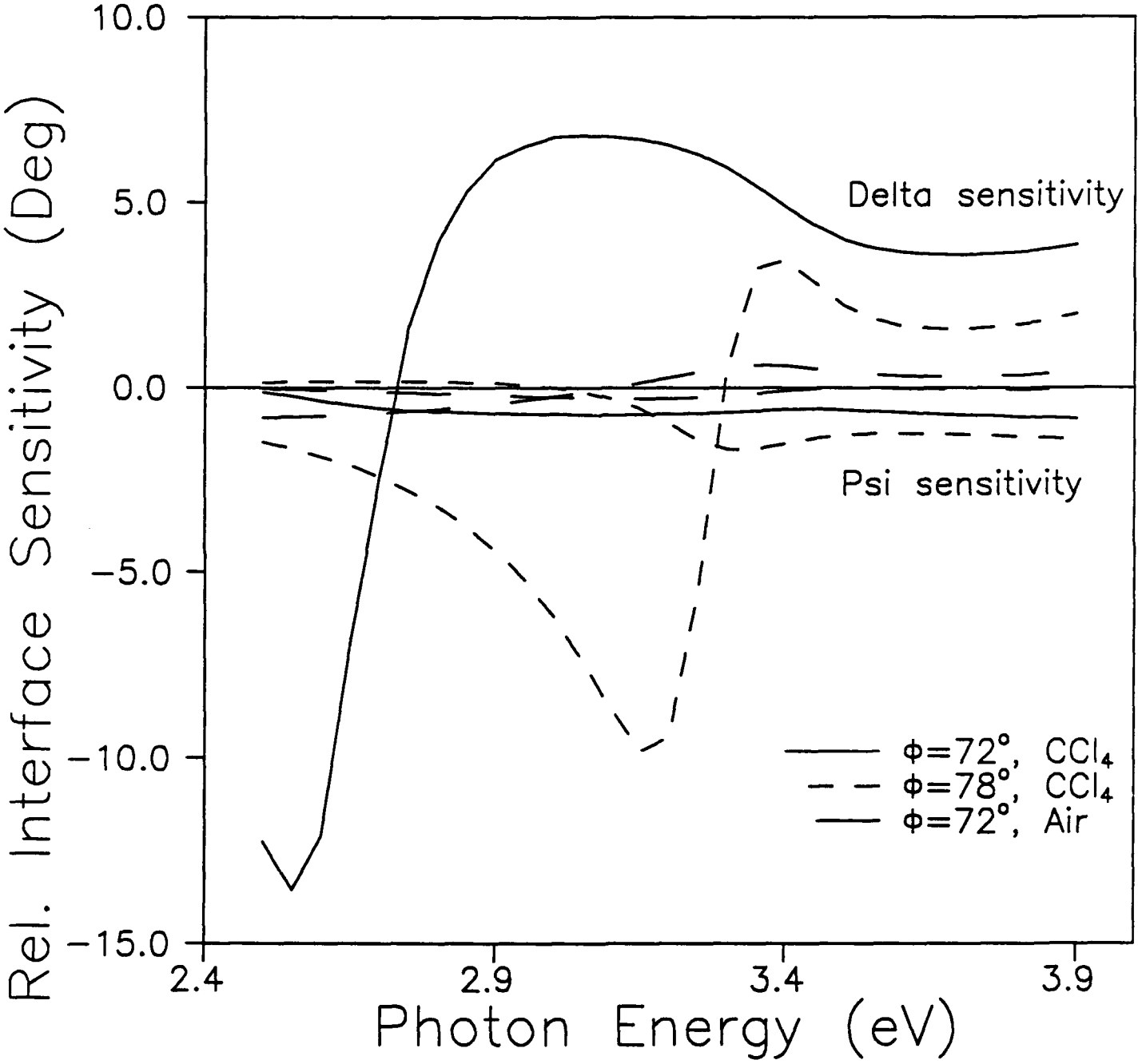

10.0
5.0
0.0
−5.0
−10.0
−15.0
Rel. Interface Sensitivity (Deg)
2.4
2.9
3.4
3.9
Photon Energy (eV)
Delta sensitivity
Psi sensitivity
Φ=72°, CCl4
Φ=78°, CCl4
Φ=72°, Air

Fig 5

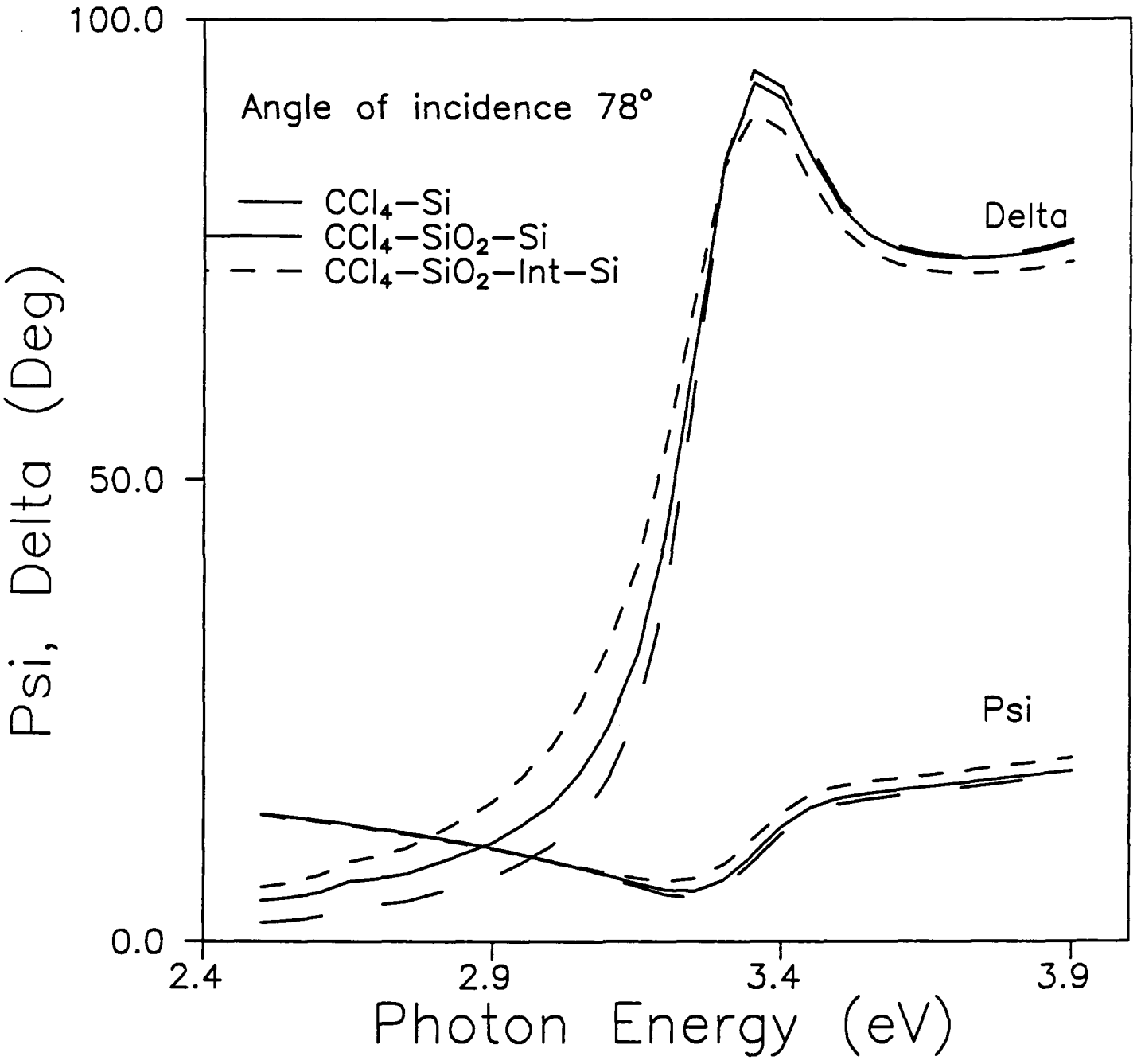
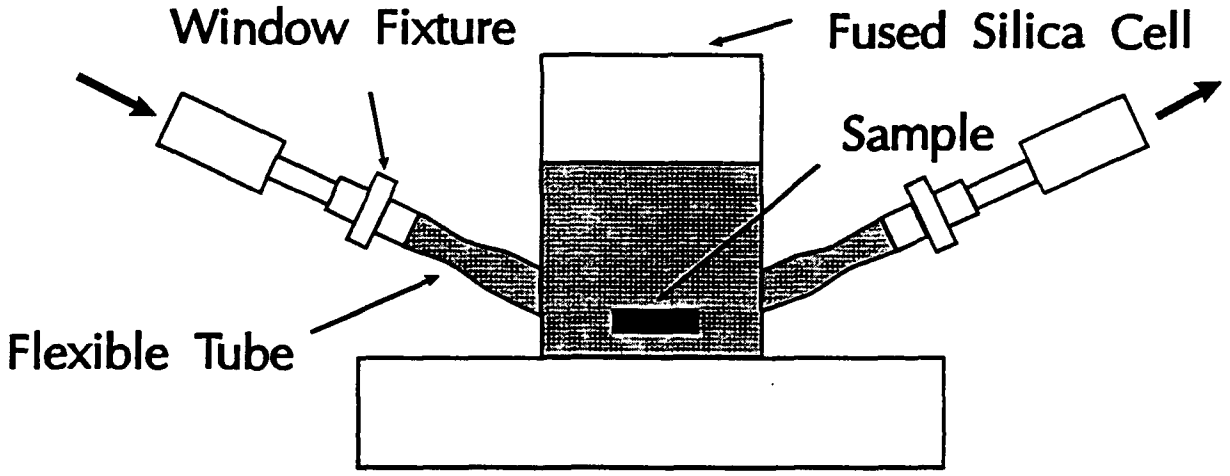

100.0
50.0
0.0
Psi, Delta (Deg)
Angle of incidence 78°
CCl4–Si
CCl4–SiO2–Si
CCl4–SiO2–Int–Si
Delta
Psi
2.4
2.9
3.4
3.9
Photon Energy (eV)

Fig 6

In-Situ Ellipsometer Immersion Cell

Polarizer Arm

Analyzer Arm



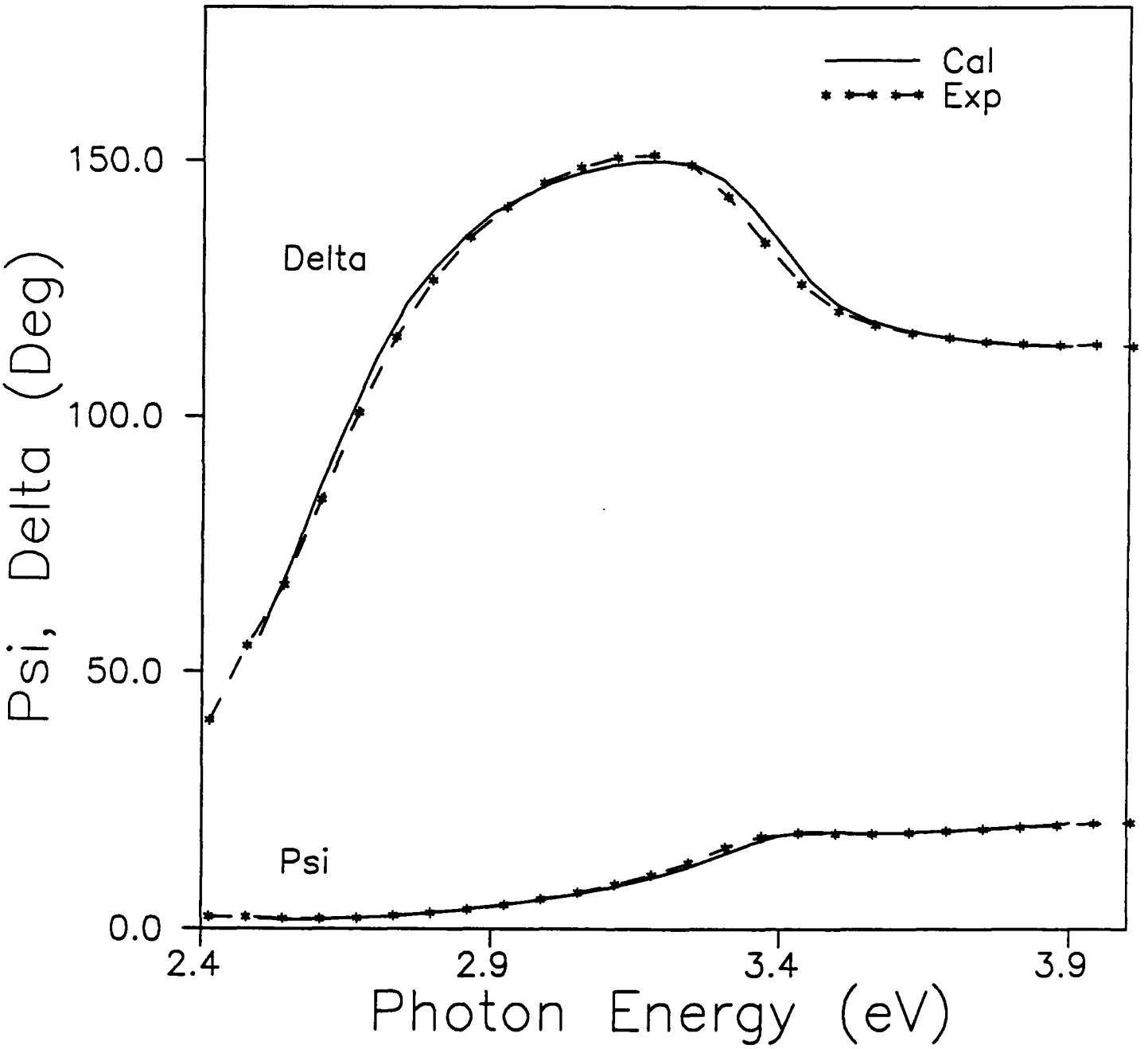

Cal
Exp
150.0
100.0
50.0
0.0
Delta
Psi
Psi, Delta (Deg)
2.4
2.9
3.4
3.9
Photon Energy (eV)

Fig 2